YMTHE, Volume *30*

Supplemental Information

Development of a double shmiR lentivirus effectively targeting both BCL11A and ZNF410 for enhanced induction of fetal hemoglobin to treat β-hemoglobinopathies

Boya Liu, Christian Brendel, Divya S. Vinjamur, Yu Zhou, Chad Harris, Meaghan McGuinness, John P. Manis, Daniel E. Bauer, Haiming Xu, and David A. Williams

Supplemental Figure

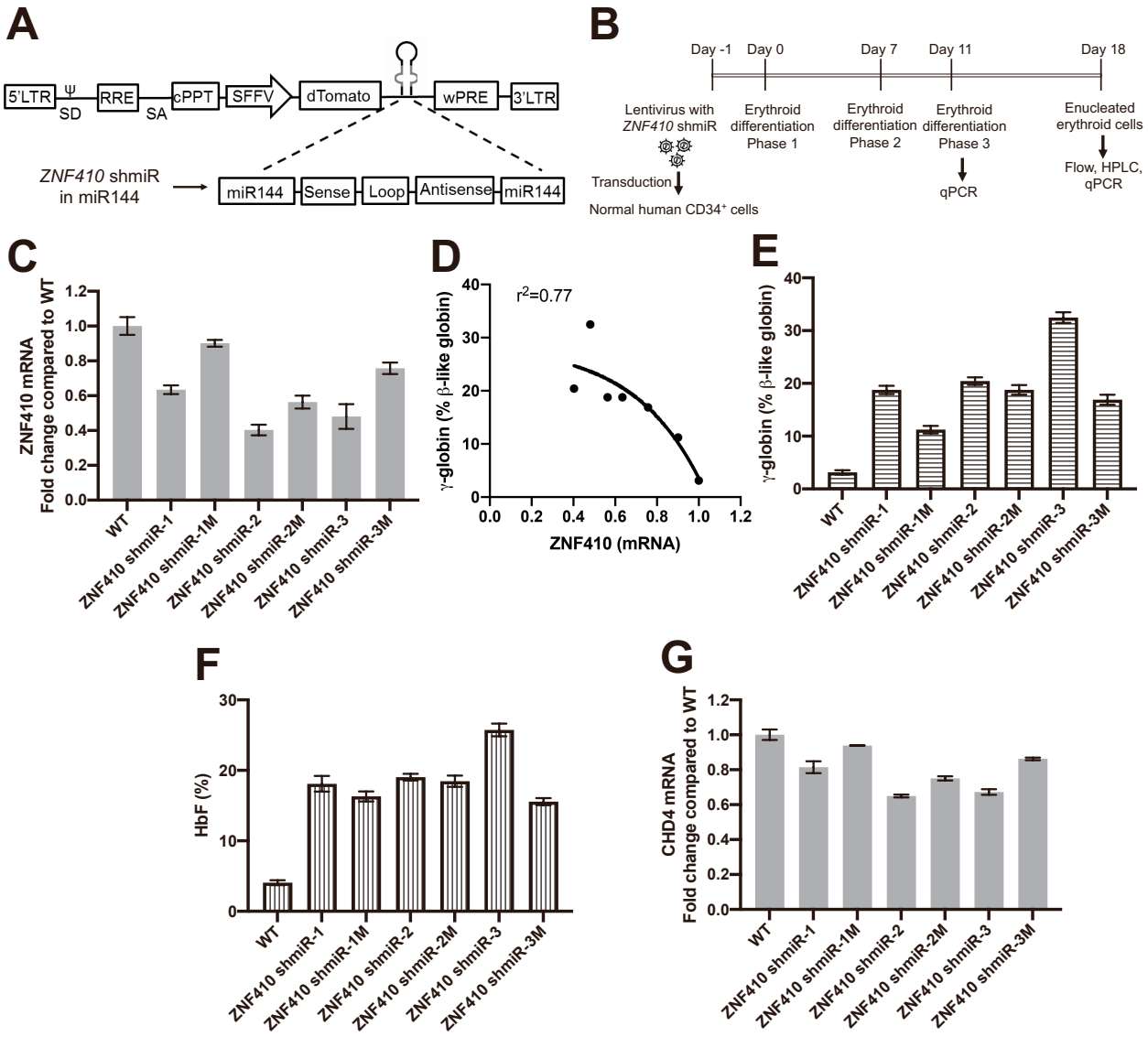

Figure S1. Identification of efficient ZNF410 shmiR for HbF induction. (A) Schematic representation of LV-SFFV-miR144 ZNF410 lentiviral vectors with shRNA targeting ZNF410. (B) Schema of virus transduction and erythroid differentiation of human CD34+ HSPCs. (C) Comparison of knockdown efficiency of ZNF410 shmiRs (labeled as 1, 1M, 2, 2M, 3 and 3M). ZNF410 expression at day 11 by RT–qPCR analysis of erythrocytes differentiated from ZNF410 shmiRs-transduced CD34+ HSPCs. Data represent mean ± SD, n = 3. (D) Correlation between the degree of knockdown of ZNF410 and induction of γ-globin in erythroid cells differentiated *in vitro* from transduced hCD34+ cells. Black dots represent samples transduced with different ZNF410 shmiR vectors, the Pearson correlation coefficient (r^2) is shown. (E) Induction of γ-globin mRNA by RT-qPCR determined on day 18 of differentiation. Data represent mean ± SD, n = 3. (F) Hemoglobin F in cell lysates measured by HPLC on day 18 of differentiation. Data represent mean ± SD, n = 3. (G) CHD4 expression by RT–qPCR analysis of erythrocytes at day 11 differentiated from ZNF410 shmiRs-transduced CD34+ HSPCs. Data represent mean ± SD, n = 3.

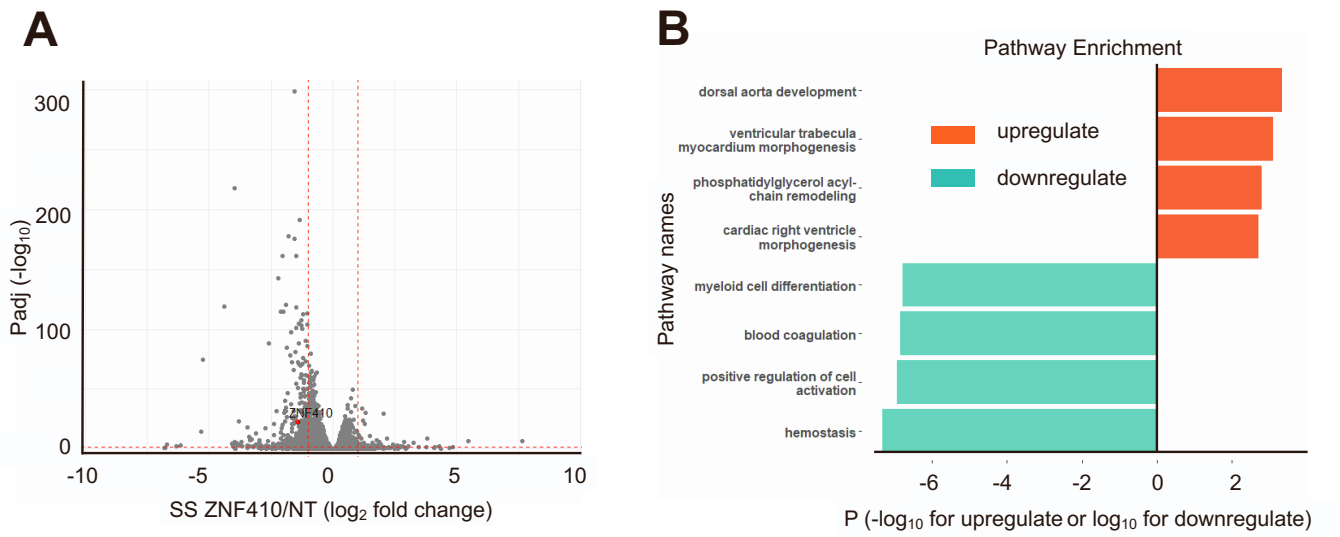

Figure S2. RNA-seq analysis of CD34+ cells transduced with ZNF410 shmiR. (A) Volcano plot of all differentially expressed genes of ZNF410 knockdown (n = 3), threshold is Padj < 0.05 and fold change >2, as red dash line showing. (B) Top 4 GO terms enriched in up or down-regulated genes, green column mean downregulated pathway, orange column mean upregulated pathway, P nominal value were calculated by $-\log_{10}$ for upregulate or $\log_{10}$ for downregulate. Phosphatidylglycerol acylchain remodeling, cardiac right ventricle morphogenesis, blood coagulation, myeloid cell differentiation.

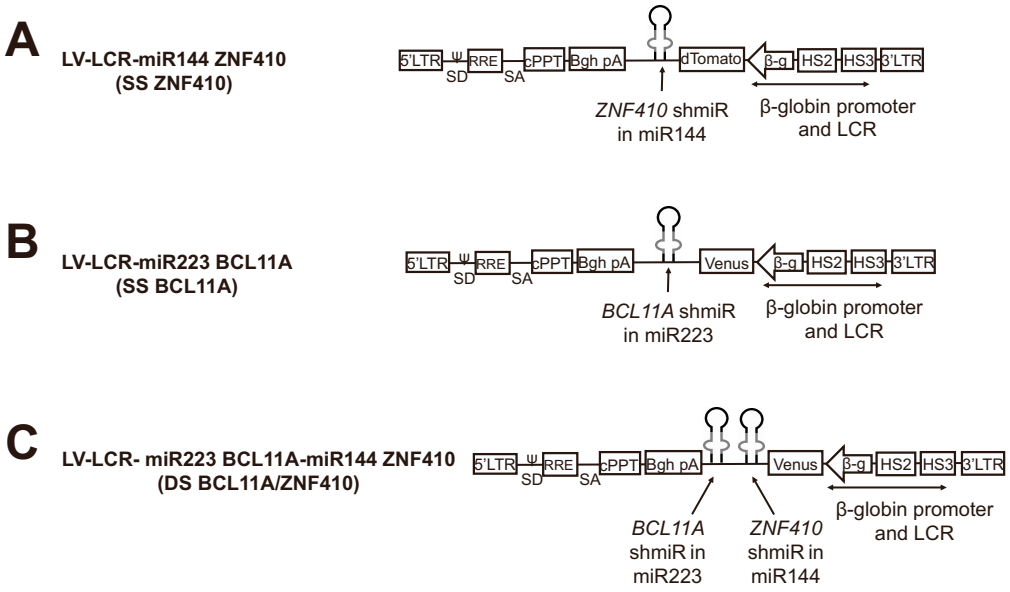

Figure S3. Lentiviral vectors used for transduction. (A) LV-LCR-miR144 ZNF410 vector (SS ZNF410), top; (B) LV-LCR-miR223 BCL11A vector (SS BCL11A), middle; and (C) double shmiR vector LV-LCR-miR223 BCL11A-miR144 ZNF410 (DS BCL11A/ZNF410), bottom.

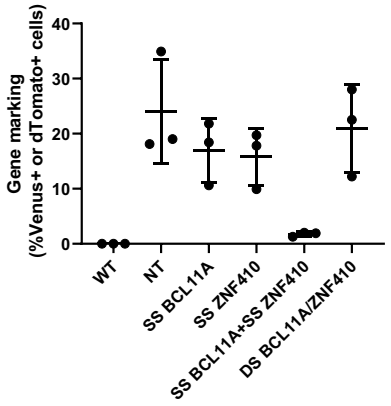

Figure S4. Gene marking of *in vitro* differentiated after transduction of human CD34+ HSPCs with shmiR vector as percent fluorescent+ cells. Data represent mean ± SD, n = 3, each data point represents an independent replicate.

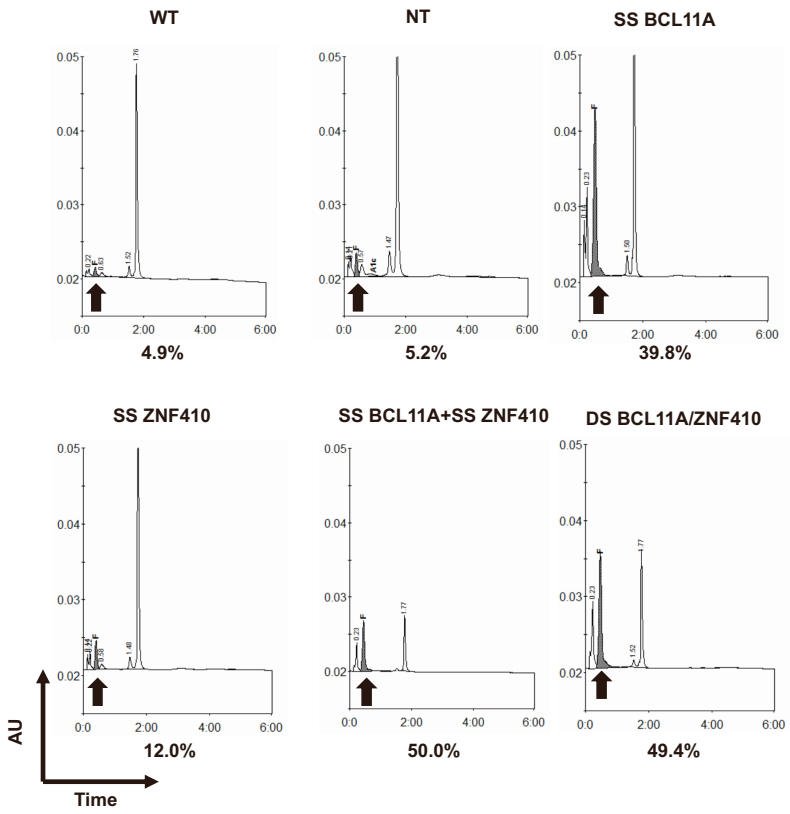

Figure S5. HPLC chromatograms of cell lysates obtained after 18 days of erythroid differentiation of transduced human CD34+ HSPCs. The arrow indicates the HbF peaks and the percentage of HbF of total hemoglobin is shown below the chromatogram.

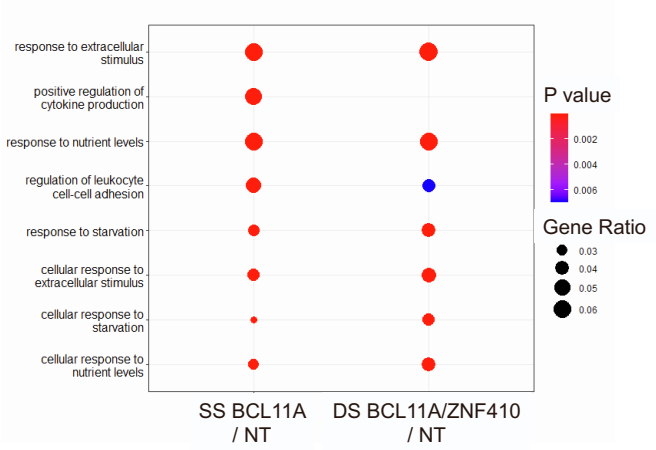

Figure S6. RNA-seq analysis of CD34+ cells transduced with SS BCL11A or DS BCL11A/ZNF410. Top 8 GO terms affected by differentially expressed genes after SS BCL11A or DS BCL11A/ZNF410 transduction. n = 3, differentially expressed genes defined by Padj < 0.05 and fold change >2.

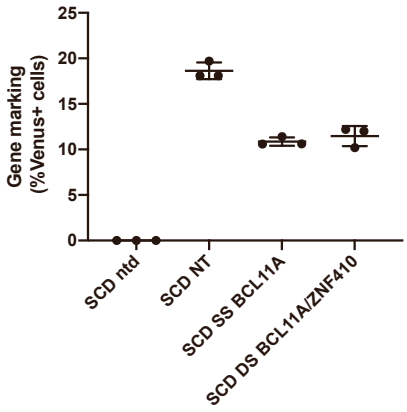

Figure S7. Gene marking of SCD patient shmiR vector transduced CD34+ HSPCs differentiated *in vitro* as a percentage of Venus+ cells. Data represent mean ± SD, n = 3, each data point represents an independent replicate.

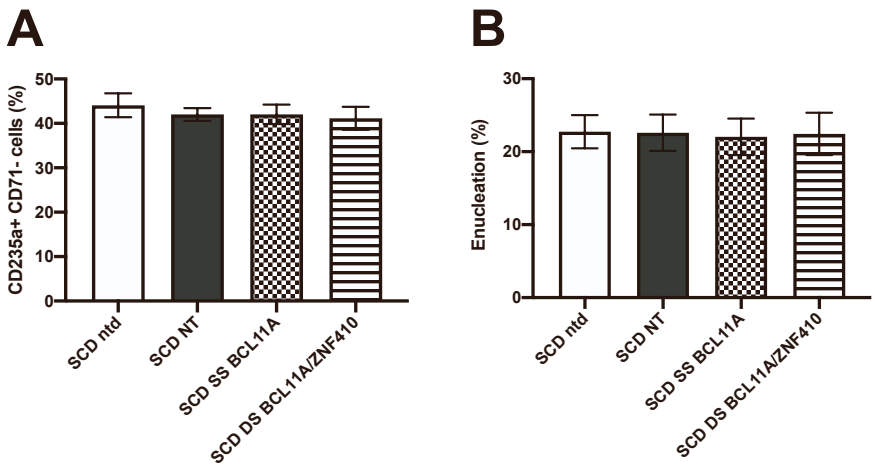

Figure S8. Effect of shmiR expression on *in vitro* erythroid differentiation and enucleation of SCD patient transduced CD34+ HSPCs. (A) Percentage of CD71-CD235a+ erythroid cells after 18 days in culture. (B) Enucleation of differentiated erythroid cells. Each data point represents an individual sample. Data represent mean ± SD, n = 3.

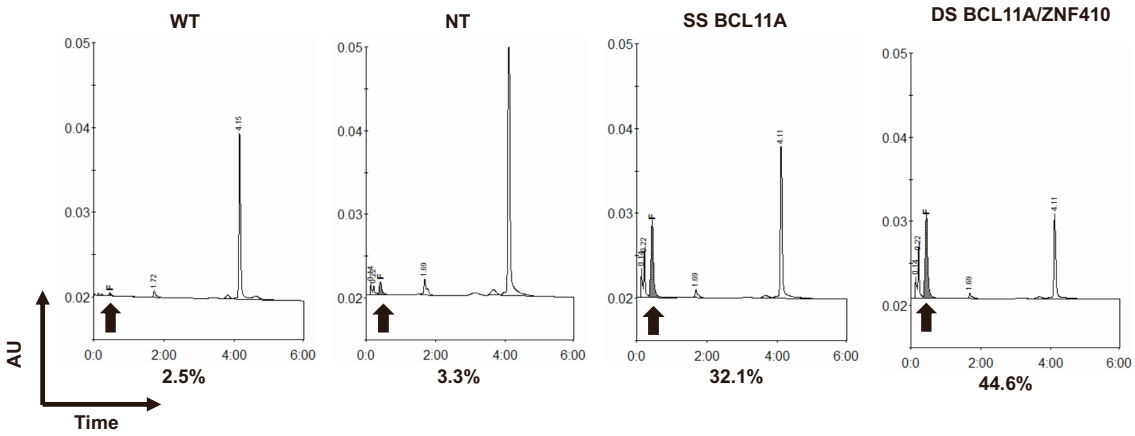

Figure S9. HPLC chromatograms of cell lysates obtained on 18 days of erythroid differentiation of transduced SCD patient CD34+ HSPCs. The arrow indicates the HbF peaks and the percentage of HbF of total hemoglobin is shown below the chromatogram.

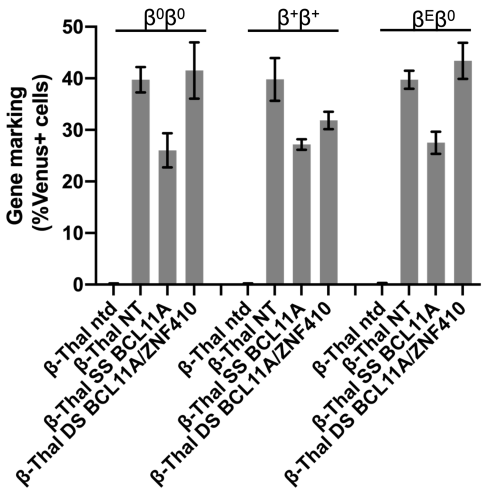

Figure S10. Gene marking of shmiR vector transduced β-thalassemia patient CD34+ HSPCs differentiated *in vitro* as a percentage of Venus+ cells. Data represent mean ± SD, n = 3, each data point represents an independent replicate.

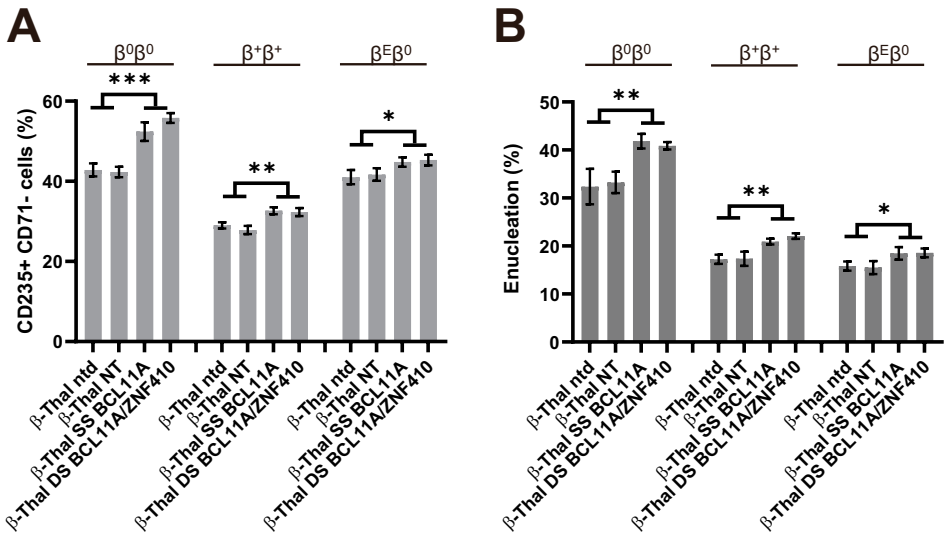

Figure S11. Effect of shmiR vector expression on *in vitro* erythroid differentiation and enucleation of transduced β-thalassemia patient CD34+ HSPCs. (A) Percentage of CD71-CD235a+ erythroid cells after 18 days in culture. (B) Enucleation of erythroid cells. Data represent mean ± SD, n = 3.

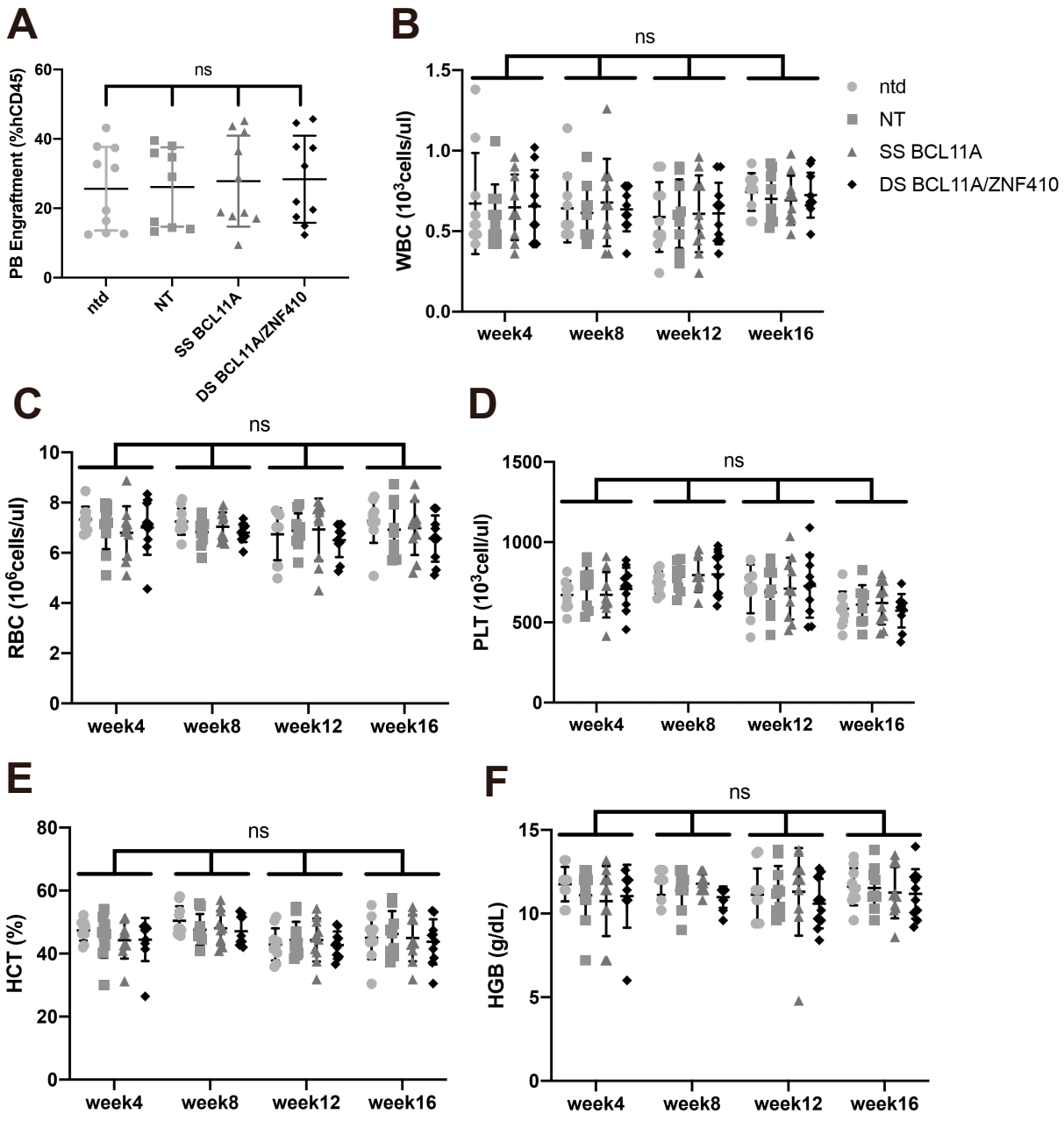

Figure S12. Peripheral blood (PB) of transplanted mice NBSGW mice analyzed at weeks 4, 8, 12 and 16. (A) Human chimerism in the PB of transplanted animals. Peripheral blood hematological parameters of transplanted animals were analyzed, including (B) white blood cell (WBC), (C) red blood cell (RBC), (D) platelet count (PLT), (E) hematocrit (HCT), (F) hemoglobin (HGB). Data represent mean ± SD, each data point represents an individual mouse. ns, not significant.

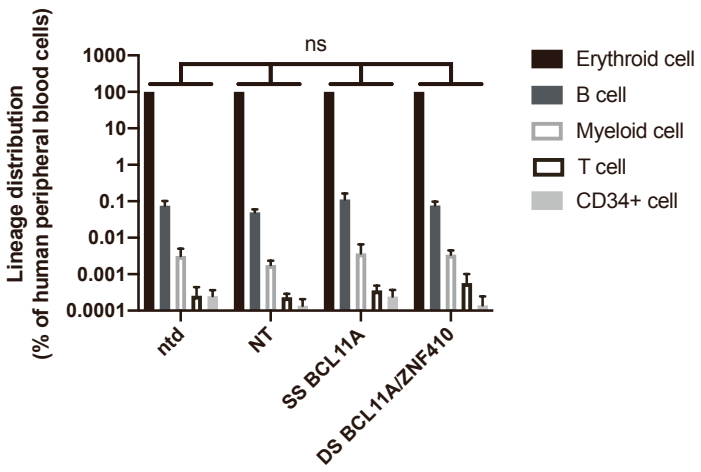

Figure S13. Hematopoietic reconstitution of transduced human CD34+ HSPCs in immunodeficient NBSGW mice. Lineage distribution of human peripheral blood (PB) cells at week 16, data represent mean ± SD.

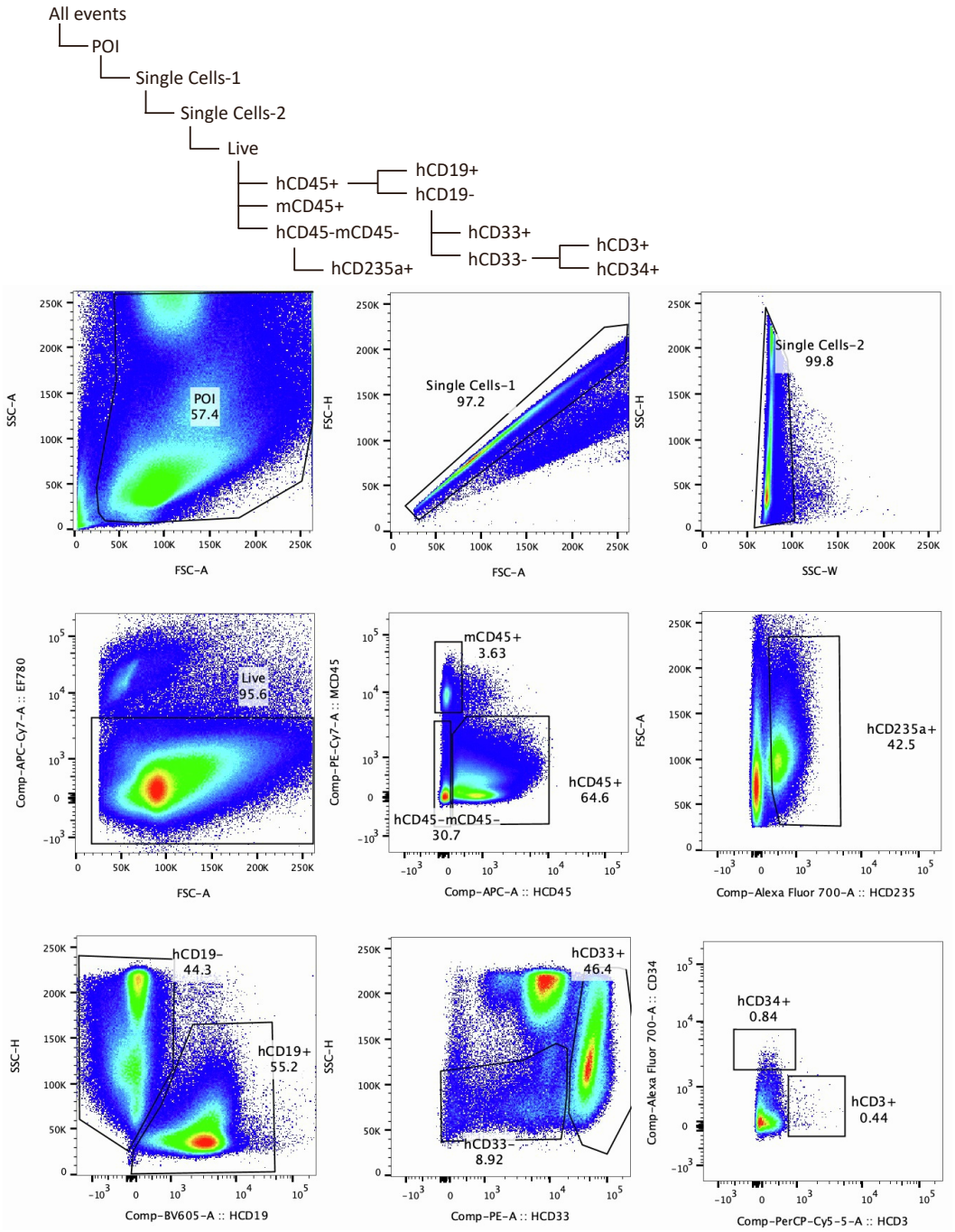

Figure S14. Representative flow cytometry analysis of bone marrow of mice after engraftment with human CD34+ cells. Hierarchy of FACS gates and representative plots for each gate are shown for a representative transplanted bone marrow sample. The first gate was plotted to delineate the cell population of interest (POI) and avoid debris. The second and third gates were plotted to exclude doublets. Values in plots are for respective gates.

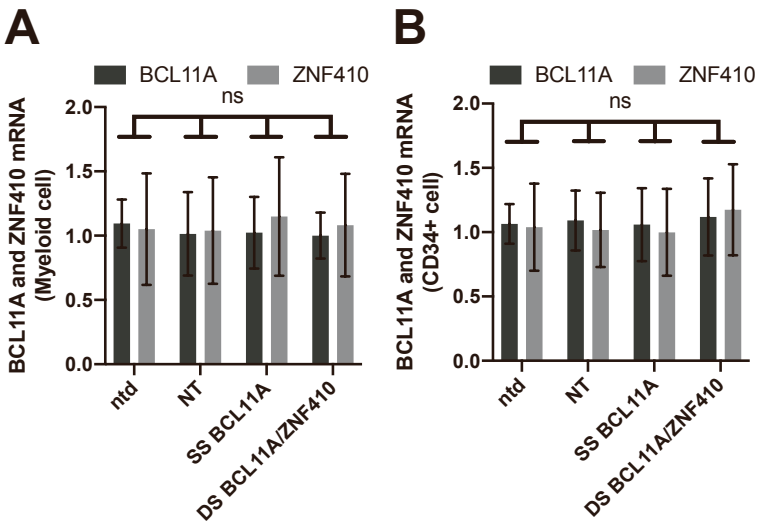

Figure S15. Gene expression analysis by RT–qPCR in human cells from BM of engrafted mice. BCL11A and ZNF410 expression normalized to GAPDH in human myeloid cells (A) and human CD34+ cells (B) sorted from BM of engrafted mice. Data represent mean ± SD, n = 10. ns, not significant.

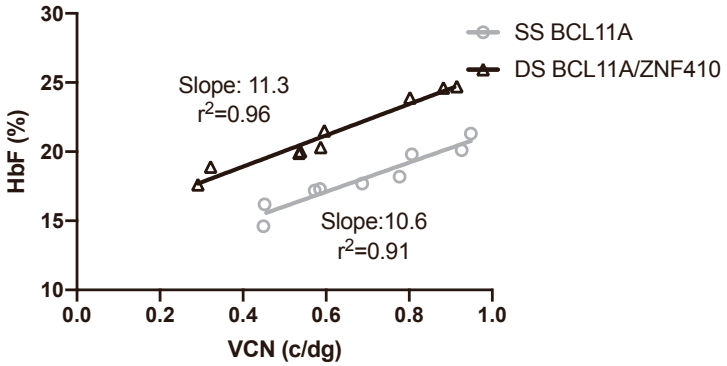

Figure S16. HbF shown in relation to VCN for SS BCL11A and DS BCL11A/ZNF410. Each data point represents an individual mouse.

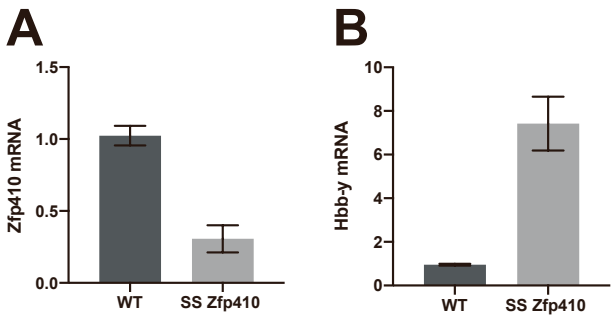

Figure S17. Efficient knockdown of Zfp410 by SS Zfp410 shmiR vector leads to high Hbb-y induction in erythroid differentiated MEL cells *in vitro*. Zfp410 (A) and Hbb-y mRNA expression as measured by RT–qPCR with Gapdh as control. Data represent mean ± SD, n = 3.

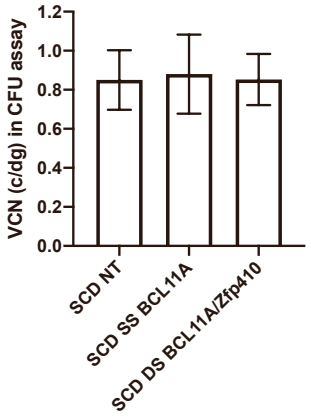

Figure S18. VCN of gene modified SCD Lin$^-$ BM cells *in vitro* before transplant by CFU. Data represent mean ± SD, n = 3.

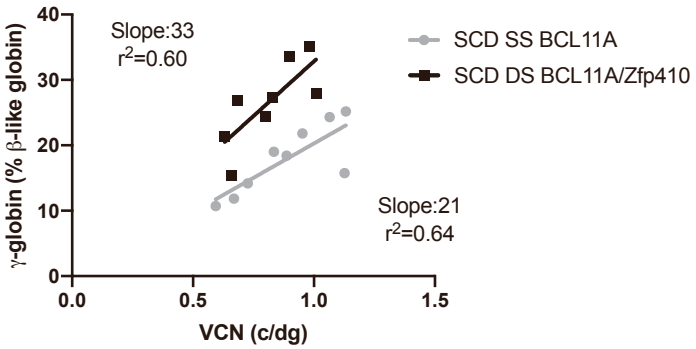

Figure S19. γ-globin of erythroid cells shown in relation to VCN for SS BCL11A and DS BCL11A/Zfp410. Each data point represents an individual mouse.

ZNF410 shmiR-1

CGCTTTTCAAGCCATGCTTCCTGTGCCCCCAGTGGGGCCCTGGCTGACCAAGGAGATTTAACTGAAAAGTTTGCGATGAGAC
ACTTTCAGTTAAATCTCCTTGGTAGTCCGGGCACCCCCAGCTCTGGAGCCTGACAAGGAGGACAGGAGAGAT

ZNF410 shmiR-1M

CGCTTTTCAAGCCATGCTTCCTGTGCCCCCAGTGGGGCCCTGGCTGGCGCACCAAGGAGATTTAACTAGTTTGCGATGAGACA
CAGTTAAATCTCCTTGGTGCGCAGTCCGGGCACCCCCAGCTCTGGAGCCTGACAAGGAGGACAGGAGAGAT

ZNF410 shmiR-2

CGCTTTTCAAGCCATGCTTCCTGTGCCCCCAGTGGGGCCCTGGCTGAAGCTCAAGTGTACAGTTGAAAGTTTGCGATGAGAC
ACTTCAACTGTACACTTGAGCTTAGTCCGGGCACCCCCAGCTCTGGAGCCTGACAAGGAGGACAGGAGAGAT

ZNF410 shmiR-2M

CGCTTTTCAAGCCATGCTTCCTGTGCCCCCAGTGGGGCCCTGGCTGGCGCAAGCTCAAGTGTACAGTAGTTTGCGATGAGAC
ACACTGTACACTTGAGCTTGCGCAGTCCGGGCACCCCCAGCTCTGGAGCCTGACAAGGAGGACAGGAGAGAT

ZNF410 shmiR-3 (SS ZNF410)

CGCTTTTCAAGCCATGCTTCCTGTGCCCCCAGTGGGGCCCTGGCTGGCTGAGCACTTAGTGTTTGTAAGTTTGCGATGAGACA
CTACAAACACTAAGTGCTCAGCAGTCCGGGCACCCCCAGCTCTGGAGCCTGACAAGGAGGACAGGAGAGAT

ZNF410 shmiR-3M

CGCTTTTCAAGCCATGCTTCCTGTGCCCCCAGTGGGGCCCTGGCTGGCGCGCTGAGCACTTAGTGTTAGTTTGCGATGAGACA
CAACACTAAGTGCTCAGCGCGCAGTCCGGGCACCCCCAGCTCTGGAGCCTGACAAGGAGGACAGGAGAGAT

SS BCL11A

GATCTCACTTCCCCACAGAAGCTCTTGGCCTGGCCTCCTGCAGTGCCACGCTGCGCGATCGAGTGTTGAATAACTCCATGTGG
TAGAGTTATTCAACACTCGATCGCGCAGTGCGGCACATGCTTACCAGCTCTAGGCCAGGGCAGATGGGATATGACGAATGGAC
TGCCAGCTGGATACAAGGATGCTCACC

DS BCL11A/ZNF410:

GATCTCACTTCCCCACAGAAGCTCTTGGCCTGGCCTCCTGCAGTGCCACGCTGCGCGATCGAGTGTTGAATAACTCCATGTGG
TAGAGTTATTCAACACTCGATCGCGCAGTGCGGCACATGCTTACCAGCTCTAGGCCAGGGCAGATGGGATATGACGAATGGAC
TGCCAGCTGGATACAAGGATGCTCACCGACGTCGACGCGTCCTCGAGGTCGCTTTTCAAGCCATGCTTCCTGTGCCCCCAGTG
GGGCCCTGGCTGGCTGAGCACTTAGTGTTTGTAAGTTTGCGATGAGACACTACAAACACTAAGTGCTCAGCAGTCCGGGCAC
CCCCAGCTCTGGAGCCTGACAAGGAGGACAGGAGAGAT

miR144 upstream sequence, ZNF410 passenger, miR144 loop, ZNF410 guide, miR144 downstream sequence
miR223 upstream sequence, BCL11A passenger, miR223 loop, BCL11A guide, miR223 downstream sequence

Figure S20. Sequence for the shmiRs (ZNF410 shmiR-1, 1M, 2, 2M, 3, 3M, SS BCL11A, DS BCL11A/ZNF410).